Available online at www.sciencedirect.com
SCIENCE DIRECT®
Journal of Solid State Chemistry 178 (2005) 2673–2679
JOURNAL OF SOLID STATE CHEMISTRY
www.elsevier.com/locate/jssc

Synthesis and characterization of two new open-framework zinc phosphites $[M(C_6N_4H_{18})][Zn_3(HPO_3)_4]$ (M = Ni, Co) with multi-directional intersecting 12-membered ring channels

Jing Liang, Jiyang Li, Jihong Yu*, Qinhe Pan, Qianrong Fang, Ruren Xu*

State Key Laboratory of Inorganic Synthesis and Preparative Chemistry, College of Chemistry, Jilin University, Changchun 130012, PR China

Received 16 April 2005; received in revised form 27 May 2005; accepted 1 June 2005
Available online 19 July 2005

Abstract

Two new open-framework zinc phosphites, $[M(C_6N_4H_{18})][Zn_3(HPO_3)_4]$ (M = Ni, Co), have been prepared under hydrothermal conditions. Single-crystal X-ray diffraction analysis shows that $[Ni(C_6N_4H_{18})][Zn_3(HPO_3)_4]$ (**1**) and $[Co(C_6N_4H_{18})][Zn_3(HPO_3)_4]$ (**2**) are isostructural and both crystallize in the monoclinic space group $C2/c$ with $a = 15.325(3)$ Å, $b = 9.792(2)$ Å, $c = 14.514(3)$ Å, $\beta = 109.83(3)^\circ$, $V = 2048.8(7)$ Å^3, $Z = 4$, $R_1 = 0.0408$ ($I > 2\sigma(I)$), and $wR_2 = 0.1104$ (all data) for **1**, and $a = 15.277(2)$ Å, $b = 9.8831(13)$ Å, $c = 14.534(2)$ Å, $\beta = 109.328(2)^\circ$, $V = 2070.7(5)$ Å^3, $Z = 4$, $R_1 = 0.0380$ ($I > 2\sigma(I)$), and $wR_2 = 0.1093$ (all data) for **2**. The structures of **1** and **2** are built up from strictly alternating ZnO_4 tetrahedra and HPO_3 pseudo-pyramids linked through oxygen vertices to form the three-dimensional (3-D) open-frameworks with multi-directional intersecting 12-membered ring (12-MR) channels. The M(TETA) (M = Ni, Co) complexes self-assembled under hydrothermal system connect with the inorganic host via M–O–P linkages and interact with inorganic framework through weak H-bonds. The two compounds show intense photoluminescence upon photoexcitation at 235 nm.

Keywords: Zinc phosphite; Hydrothermal synthesis; Open-framework; Crystal structure

1. Introduction

Over the past few decades, open-framework metal phosphates have been intensively investigated due to their rich structural chemistry and potential applications in the catalyses, separations and ion-exchange processes [1-4]. In particular, the growing family of open-framework zinc phosphates exhibit fascinating structural characters [5-9], such as $[NH_3(CH_2)_2NH_2(CH_2)_2NH_3]Zn_4(PO_4)_3(HPO_4)\cdot H_2O$ [8] and $Co(dien)_2Zn_2(HPO_4)_4\cdot H_3O$ [9] with intersecting helical channels.

Recently, the replacement of tetrahedral phosphate groups by pyramidal phosphite units has resulted in the preparation of a new class of metal phosphite compounds with interesting structural architectures, including 0-D cluster, 1-D chain, 2-D layer and 3-D open-framework structures [10-24]. A number of zinc phosphites have been prepared under hydrothermal conditions [14-24]. In general, their inorganic hosts are built up from Zn-centered tetrahedra (ZnO_4 or ZnO_3N) and P-centered $HP^{III}O_3^{2-}$ pseudo-pyramids. Examples for these compounds are known as 0-D cluster $C_4N_3OH_7\cdot Zn(H_2O)HPO_3$ [14], 1-D chain $H_3N(CH_2)_3NH_3\cdot Zn(HPO_3)_2$ [15], 2-D layers $(C_5H_6N_2)Zn(HPO_3)$ [16] and $[H_2N(CH_2)NH_2]_{0.5}\cdot ZnHPO_3$ [17], and 3-D open-frameworks $(NC_5H_{12})_2Zn_3(HPO_3)_4$ [18] and $[CN_3H_6]_2Zn(HPO_3)_2$ [19].

Open-framework metal phosphates containing heteroatoms are of particular interest for their wide applications in catalytic processes. For example, nickel-containing silicoaluminophosphate (SAPO-34) is one

*Corresponding author. Fax: +86 431 516 8608.
E-mail address: jihong@mail.jlu.edu.cn (J. Yu).

0022-4596/$ - see front matter © 2005 Elsevier Inc. All rights reserved.
doi:10.1016/j.jssc.2005.06.002

of the best catalysis for methanol to olefin (MTO) conversion yielding close to 90% ethene at a reaction temperature of 450 °C [25]. However, little success has been made to incorporate the heteroatoms into the open-frameworks of metal phosphites. More recently, a novel nickel–zinc phosphite $Ni(DETA)(H_2O)Zn_2(HPO_3)_3$ (FJ-14) with intersecting 3-D 16-MR channels has been hydrothermally prepared [26]. In its structure, the zinc phosphite layers are pillared by $Ni_2(DETA)_2(H_2O)_2O_2$ dinuclear units to generate a 3-D framework (DETA = diethylenetriamine).

In the present work, two new zinc phosphites $[M(TETA)][Zn_3(HPO_3)_4]$ (M = Ni, Co; TETA = triethylenetetramine) have been hydrothermally synthesized by using H_3PO_3 as the phosphorus source. Their open-framework structures contain multi-directional intersecting 12-MR channels, and their photoluminescent properties have been discussed.

2. Experimental section

2.1. Materials and methods

All reagents were purchased commercially and used without further purification. The X-ray powder diffraction (XRD) data were collected on a Siemens D5005 diffractometer with Cu$K\alpha$ radiation ($\lambda = 1.5418$ Å). Infrared spectra were recorded on a Nicolet Impact 410 FT-IR spectrometer using KBr pellets. Inductively coupled plasma (ICP) analysis was performed on a Perkin-Elmer Optima 3300DV spectrometer. Elemental analysis was conducted on a Perkin-Elmer 2400 elemental analyzer. A Perkin-Elmer TGA 7 unit was used to carry out the thermogravimetric analysis (TGA) in the air with a heating rate of 20 °C/min. Fluorescence spectroscopy data were recorded on a LS55 luminescence spectrometer.

2.2. Synthesis of $[Ni(C_6N_4H_{18})][Zn_3(HPO_3)_4]$, 1

In a typical synthesis of **1**, a reaction mixture of ZnO (0.36 g), $NiCl_2 \cdot 6H_2O$ (0.79 g), TETA (1.32 mL), H_3PO_3 (0.725 g) and H_2O (10 mL) in a molar ratio of 1.0:0.75:2.0:2.0:126 was stirred under ambient condition. The formed homogenous gel with a pH value about 6.5 was sealed in a Teflon-lined stainless steel autoclave and heated at 160 °C for 120 h under static condition. The solid product consisting of large single crystals in the form of light-blue prisms was obtained by filtration, washed by distilled water and then dried in the oven at 100 °C. The ICP and elemental analysis results of **1** were consistent with the theoretical values based on the crystal data. Found for **1**: Zn, 26.55; Ni, 7.65; P, 16.5; C, 9.94; H, 2.95; N, 7.74 wt%. Calcd: Zn, 27.20; Ni, 8.14; P, 17.18; C, 10.00; H, 3.08; N, 7.77 wt%.

2.3. Synthesis of $[Co(C_6N_4H_{18})][Zn_3(HPO_3)_4]$, 2

In the synthesis of **2**, a reaction mixture of ZnO (0.36 g), $CoCl_2 \cdot 6H_2O$ (0.79 g), TETA (0.66 mL), H_3PO_3 (0.653 g) and H_2O (10 mL) in a molar ratio of 1.0:0.75:1.0:1.8:126 was stirred under ambient condition. The formed homogeneous reaction mixture with a pH value about 6.0 was sealed in a Teflon-lined stainless steel autoclave and heated at 160 °C for 120 h under static condition. The resulting product consisting of large single crystals in the form of purple prisms was filtered, washed with distilled water and dried in the oven at 100 °C. The ICP and elemental analysis results of **2** were in good agreement with the theoretical values. Found for **2**: Zn, 26.95; Co, 7.95; P, 17.01; C, 9.93; H, 2.98; N, 7.70 wt%. Calcd: Zn, 27.19; Co, 8.17; P, 17.18; C, 9.99; H, 3.07; N, 7.77 wt%.

2.4. Determination of crystal structure

Crystals with dimensions $0.15 \times 0.12 \times 0.12\,mm^3$ for **1** and $0.16 \times 0.13 \times 0.13\,mm^3$ for **2** were selected for single-crystal XRD analysis, respectively. The intensity data were collected on a Siemens SMART CCD diffractometer using graphite-monochromatic Mo$K\alpha$ radiation ($\lambda = 0.71073$ Å) at a temperature of 20 ± 2 °C. Data processing was accomplished with the SAINT processing program [27]. Both structures were solved by direct methods with the SHELXTL software package [28]. The zinc, nickel and phosphorus atoms for **1** and zinc, cobalt, phosphorus atoms for **2** were determined directly, and carbon, nitrogen and oxygen were subsequently found in the difference Fourier map. The C(3) atom in **1** and **2** was found to be disordered over two positions with an equal occupancy, so the H atoms associated with C(3), C(3′), C(2) and N(2) atoms were not located. Other H atoms residing on the TETA molecules were placed geometrically. The H atoms of HPO_3 groups were found in the final difference Fourier map. All non-hydrogen atoms were refined with anisotropic thermal parameters. Experimental details for the structure determinations of the compounds **1** and **2** are presented in Table 1.

3. Results and discussion

3.1. Characterization

As seen in Fig. 1, the XRD patterns of **1** and **2** are similar, suggesting that their structures might be analogous. Furthermore, their diffraction peaks are consistent with the simulated one generated on the basis of single-crystal structural data of **1**, indicating the purity of the as-synthesized products. The differences in

Table 1
Crystal data and structure refinement for the title compounds **1** and **2**

Compound	$Ni(C_6N_4H_{18})Zn_3(HPO_3)_4$ (**1**)		$Co(C_6N_4H_{18})Zn_3(HPO_3)_4$ (**2**)	
Empirical formula	$C_6H_{22}N_4NiO_{12}P_4Zn_3$		$C_6H_{22}N_4CoO_{12}P_4Zn_3$	
Formula weight	720.98		721.20	
Temperature (K)	293(2)		293(2)	
Wavelength (Å)	0.71073		0.71073	
Crystal system, space group	Monoclinic, $C2/c$		Monoclinic, $C2/c$	
Unit cell dimensions	$a = 15.325(3)$ Å	$\alpha = 90^\circ$	$a = 15.277(2)$ Å	$\alpha = 90^\circ$
	$b = 9.792(2)$ Å	$\beta = 109.83(3)^\circ$	$b = 9.8831(13)$ Å	$\beta = 109.328(2)^\circ$
	$c = 14.514(3)$ Å	$\gamma = 90^\circ$	$c = 14.534(2)$ Å	$\gamma = 90^\circ$
Volume ($Å^3$)	2048.8(7)		2070.7(5)	
Z, calculated density (Mg/m^3)	4, 2.337		4, 2.313	
Absorption coefficient (mm^{-1})	4.752		4.594	
$F(000)$	1440		1436	
Crystal size (mm^3)	$0.15 \times 0.12 \times 0.12$		$0.16 \times 0.13 \times 0.13$	
Theta range for data collection (deg)	2.51–27.89		2.50–28.15	
Limiting indices	$-19 \leqslant h \leqslant 10$, $-12 \leqslant k \leqslant 11$, $-17 \leqslant l \leqslant 18$		$-20 \leqslant h \leqslant 16$, $-10 \leqslant k \leqslant 12$, $-11 \leqslant l \leqslant 19$	
Reflections collected/unique	5808/2235 [R (int) = 0.0606]		5989/2324 [R (int) = 0.0946]	
Completeness to $\theta = 27.35$	91.6%		91.7%	
Refinement method	Full-matrix least-squares on F^2		Full-matrix least-squares on F^2	
Data/restraints/parameters	2235/0/155		2324/0/160	
Goodness-of-fit on F^2	1.023		1.060	
Final R indices [$I > 2\sigma(I)$][a]	$R_1 = 0.0408$, $wR_2 = 0.1083$		$R_1 = 0.0380$, $wR_2 = 0.1081$	
R indices (all data)	$R_1 = 0.0434$, $wR_2 = 0.1104$		$R_1 = 0.0394$, $wR_2 = 0.1093$	
Largest diff. peak and hole	1.038 and -1.127 e $Å^{-3}$		0.788 and -0.900 e $Å^{-3}$	

[a] $R_1 = \sum ||F_o| - |F_c|| / \sum |F_o|$. $wR_2 = \{\sum[w(F_o^2 - F_c^2)^2] / \sum[w(F_o^2)^2]\}^{1/2}$.

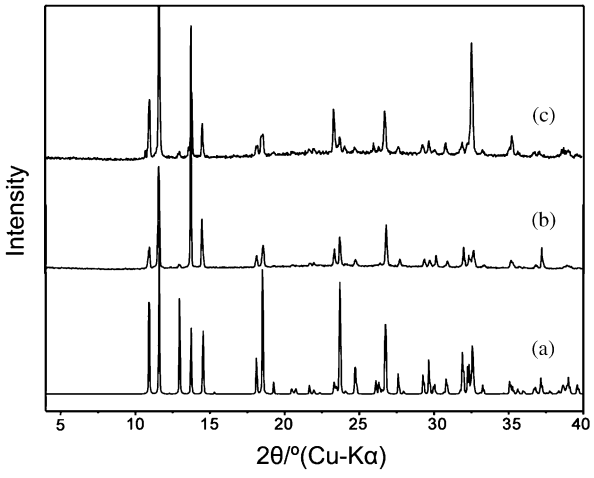

Fig. 1. XRD patterns: (a) simulated from crystal structure data of **1**; (b) as-synthesized compound **1**; (c) as-synthesized compound **2**.

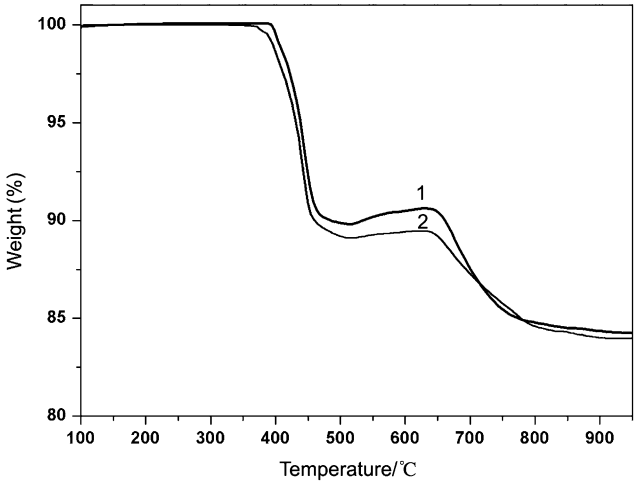

Fig. 2. Thermogravimetric curves of **1** and **2**.

reflection intensity are probably due to preferred orientations in the powder samples.

Thermogravimetric curves of **1** and **2** are given in Fig. 2. TG analysis for **1** shows two stages of weight loss in a total of 16.50 wt% around 400–950 °C, which is attributed to the decomposition of TETA molecules (calcd. 20.25 wt% for one TETA molecule per formula unit), the dehydration (calcd. 4.99 wt% for two water molecules per formula unit), and the weight increase corresponding to aerial oxidation of phosphite to phosphate (calcd. 8.88 wt%) [29]. XRD analysis indicates that the structure of **1** becomes amorphous after the decomposition of TETA molecules above 400 °C. TG analysis for **2** also shows a two-step weight loss of 16.81 wt% between 390 and 950 °C, which is assigned to the removal of TETA ligands (calcd. 20.24 wt% for one TETA molecule per formula unit), the dehydration (calcd. 4.99 wt% for two water molecules per formula

unit), and the weight increase due to aerial oxidation of phosphite to phosphate (calcd. 8.87 wt%). XRD analysis indicates that the structure of **2** becomes amorphous above 400 °C.

3.2. Structure determination of 1 and 2

Single-crystal XRD analysis of compounds **1** and **2** reveals that they are identical in the structures with the empirical formula of $[M(C_6N_4H_{18})][Zn_3(HPO_3)_4]$ (M = Ni, Co). The asymmetric unit of **1**, as seen in Fig. 3, contains two crystallographically distinct phosphorus atoms. P(1) connects three O atoms with nearby Zn atoms [P(1)–O: 1.507(3)–1.515(3) Å], leaving a terminal P–H bond of 1.28(5) Å. P(2) makes two P–O–Zn bonds and one P–O–Ni bond with Zn and Ni atoms [P(2)–O: 1.502(3)–1.530(3) Å], and has a terminal P–H bond of 1.30(5) Å. The existence of P–H bonds is also confirmed by the characteristic band of phosphite groups [ν(H-P), 2380 cm^{-1}] in the IR spectrum [11,12]. The Zn atoms occupy two crystallographic sites. The Zn(1) atom is tetrahedrally coordinated by oxygen atoms with Zn(1)–O bond lengths within 1.912(3)–1.953(3) Å, and O–Zn(1)–O angles within 104.05(14)–118.01(14)°. The Zn(2) atom locates on the two-fold axis and shares two μ-O atoms with adjacent P atoms [Zn(2)–O: 1.903(3) Å] and two μ_3-O atoms with adjacent Ni atoms [Zn(2)–O: 1.984(3) Å]. The Ni atom located on the two-fold axis is six-coordinated with two framework oxygen atoms in *cis*-position and four nitrogen atoms of one TETA ligand [Ni–O: 2.179(3) Å and Ni–N: 2.082(4)–2.102(4) Å]. The TETA molecule acts as a tetradentate ligand bonded to the Ni center. The coordination mode of organic amine TETA and Ni atom assembled under hydrothermal conditions is similar to those observed in $Ni(DETA)(H_2O)Zn_2(HPO_3)_3$ [26] and $[Ga_2(DETA)(PO_4)_2]\cdot 2H_2O$ (NTHU-1) [30]. The asymmetric unit of **2** is similar to that of **1**, in which nickel atom is replaced by cobalt atom. The selected bond lengths and angles, and the atomic coordinates of compounds **1** and **2** are shown clearly in Tables 2–5, respectively.

In the structures of compounds **1** and **2**, the alternating connection of ZnO_4 and HPO_3 units forms the 2-D sheets with 4.12-net parallel to the *ac* plane. The M(TETA) (M = Ni, Co) complexes are incorporated into 12-MR via μ_3-O atoms to form P–O–M linkages. The zinc phosphite layers are stacked along the [010] direction in an AAAA sequence and they are further connected with each other through O(2) atoms to generate the 3-D open-frameworks of **1** and **2** (Fig. 4).

The open-frameworks of compounds **1** and **2** contain multi-directional 12-MR channels. Fig. 5 shows the framework viewed along the [100] and [001] directions. It contains 12-MR channels and the atom-to-atom dimensions of these two kinds of 12-MR windows are

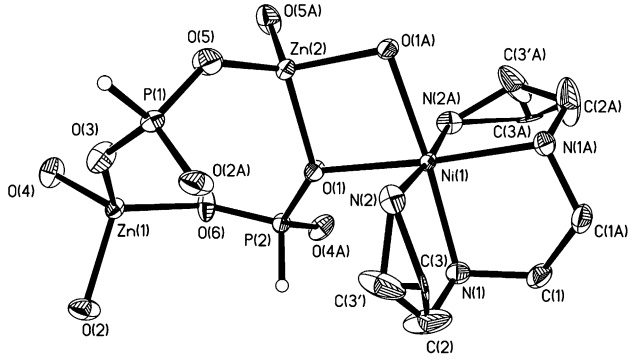

Fig. 3. Thermal ellipsoid plot (50%) for **1** showing the asymmetric unit and atomic labeling scheme.

Table 2
Selected bond lengths (Å) and bond angles (°) for **1**

Zn(1)–O(3)	1.912(3)	P(1)–H(1)	1.28(5)
Zn(1)–O(4)	1.932(3)	P(2)–O(4)#3	1.502(3)
Zn(1)–O(6)	1.942(3)	P(2)–O(6)	1.513(3)
Zn(1)–O(2)	1.953(3)	P(2)–O(1)	1.530(3)
Zn(2)–O(5)	1.903(3)	P(2)–H(2)	1.30(5)
Zn(2)–O(5)#1	1.903(3)	Ni(1)–N(2)	2.082(4)
Zn(2)–O(1)#1	1.984(3)	Ni(1)–N(2)#1	2.082(4)
Zn(2)–O(1)	1.984(3)	Ni(1)–N(1)#1	2.102(4)
P(1)–O(5)	1.507(3)	Ni(1)–N(1)	2.102(4)
P(1)–O(3)	1.511(3)	Ni(1)–O(1)	2.179(3)
P(1)–O(2)#2	1.515(3)	Ni(1)–O(1)#1	2.179(3)
N(2)–Ni(1)–N(2)#1	174.2(2)	O(5)–Zn(2)–O(1)	112.26(14)
N(2)–Ni(1)–N(1)#1	101.14(14)	O(5)#1–Zn(2)–O(1)	111.87(15)
N(2)#1–Ni(1)–N(1)#1	83.22(15)	O(1)#1–Zn(2)–O(1)	89.48(17)
N(2)–Ni(1)–N(1)	83.22(15)	O(5)–P(1)–O(3)	114.2(2)
N(2)#1–Ni(1)–N(1)	101.14(14)	O(5)–P(1)–O(2)#2	112.0(2)
N(1)#1–Ni(1)–N(1)	84.8(2)	O(3)–P(1)–O(2)#2	113.37(19)
N(2)–Ni(1)–O(1)	86.88(14)	O(5)–P(1)–H(1)	106(2)
N(2)#1–Ni(1)–O(1)	88.64(14)	O(3)–P(1)–H(1)	106(2)
N(1)#1–Ni(1)–O(1)	171.73(13)	O(2)#2–P(1)–H(1)	104(2)
N(1)–Ni(1)–O(1)	98.32(13)	O(4)#3–P(2)–H(2)	108(2)
N(2)–Ni(1)–O(1)#1	88.64(14)	O(6)–P(2)–H(2)	107(2)
N(2)#1–Ni(1)–O(1)#1	86.88(14)	O(1)–P(2)–H(2)	106(2)
N(1)#1–Ni(1)–O(1)#1	98.32(13)	O(4)#3–P(2)–O(6)	112.19(19)
N(1)–Ni(1)–O(1)#1	171.73(13)	O(4)#3–P(2)–O(1)	112.30(19)
O(1)–Ni(1)–O(1)#1	79.71(15)	O(6)–P(2)–O(1)	110.86(18)
O(3)–Zn(1)–O(4)	110.71(14)	P(2)–O(1)–Zn(2)	130.86(18)
O(3)–Zn(1)–O(6)	118.01(14)	P(2)–O(1)–Ni(1)	130.98(17)
O(4)–Zn(1)–O(6)	105.64(14)	Zn(2)–O(1)–Ni(1)	95.41(12)
O(3)–Zn(1)–O(2)	107.92(16)	P(1)#2–O(2)–Zn(1)	126.7(2)
O(4)–Zn(1)–O(2)	104.05(14)	P(1)–O(3)–Zn(1)	138.0(2)
O(6)–Zn(1)–O(2)	109.64(16)	P(2)#4–O(4)–Zn(1)	142.6(2)
O(5)–Zn(2)–O(5)#1	116.1(2)	P(1)–O(5)–Zn(2)	133.6(2)
O(5)–Zn(2)–O(1)#1	111.87(15)	P(2)–O(6)–Zn(1)	135.7(2)
O(5)#1–Zn(2)–O(1)#1	112.26(14)		

Symmetry transformations used to generate equivalent atoms: #1 $-x+1, y, -z+1/2$; #2 $-x+1/2, -y+1/2, -z$; #3 $-x+1/2, y+1/2, -z+1/2$; #4 $-x+1/2, y-1/2, -z+1/2$.

Table 3
Selected bond lengths (Å) and bond angles (°) for **2**

Zn(1)–O(3)	1.912(3)	P(1)–H(1)	1.37(3)
Zn(1)–O(4)	1.928(2)	P(2)–O(4)#3	1.502(3)
Zn(1)–O(6)	1.942(2)	P(2)–O(6)	1.515(2)
Zn(1)–O(2)	1.955(3)	P(2)–O(1)	1.527(3)
Zn(2)–O(5)	1.900(3)	P(2)–H(2)	1.39(4)
Zn(2)–O(5)#1	1.900(3)	Co(1)–N(2)	2.122(3)
Zn(2)–O(1)#1	1.988(2)	Co(1)–N(2)#1	2.122(3)
Zn(2)–O(1)	1.988(2)	Co(1)–N(1)#1	2.159(3)
P(1)–O(5)	1.508(3)	Co(1)–N(1)	2.159(3)
P(1)–O(3)	1.508(3)	Co(1)–O(1)	2.208(2)
P(1)–O(2)#2	1.516(3)	Co(1)–O(1)#1	2.208(2)
N(2)#1–Co(1)–N(2)	172.15(17)	O(5)–Zn(2)–O(1)	111.87(12)
N(2)#1–Co(1)–N(1)	104.25(12)	O(5)#1–Zn(2)–O(1)	111.21(13)
N(2)#1–Co(1)–N(1)#1	81.77(12)	O(1)#1–Zn(2)–O(1)	90.38(14)
N(2)–Co(1)–N(1)	81.77(12)	O(5)–P(1)–O(3)	114.21(18)
N(2)–Co(1)–N(1)#1	104.25(12)	O(5)–P(1)–O(2)#2	111.86(16)
N(1)–Co(1)–N(1)#1	82.46(16)	O(3)–P(1)–O(2)#2	113.07(15)
N(2)#1–Co(1)–O(1)#1	85.72(11)	O(5)–P(1)–H(1)	106.8(14)
N(2)–Co(1)–O(1)#1	88.24(11)	O(3)–P(1)–H(1)	107.0(14)
N(1)–Co(1)–O(1)#1	170.01(11)	O(2)#2–P(1)–H(1)	102.9(13)
N(1)#1–Co(1)–O(1)#1	99.95(10)	O(4)#3–P(2)–H(2)	108.3(15)
N(2)#1–Co(1)–O(1)	88.24(11)	O(6)–P(2)–H(2)	107.5(16)
N(2)–Co(1)–O(1)	85.72(11)	O(1)–P(2)–H(2)	105.1(15)
N(1)–Co(1)–O(1)	99.95(10)	O(4)#3–P(2)–O(6)	111.84(15)
N(1)#1–Co(1)–O(1)	170.01(11)	O(4)#3–P(2)–O(1)	112.44(16)
O(1)#1–Co(1)–O(1)	79.36(13)	O(6)–P(2)–O(1)	111.23(15)
O(3)–Zn(1)–O(4)	109.97(11)	P(2)–O(1)–Zn(2)	131.72(14)
O(3)–Zn(1)–O(6)	117.66(12)	P(2)–O(1)–Co(1)	130.89(14)
O(4)–Zn(1)–O(6)	105.99(11)	Zn(2)–O(1)–Co(1)	95.13(10)
O(3)–Zn(1)–O(2)	107.54(12)	P(1)#2–O(2)–Zn(1)	126.16(16)
O(4)–Zn(1)–O(2)	105.06(11)	P(1)–O(3)–Zn(1)	139.10(18)
O(6)–Zn(1)–O(2)	109.93(13)	P(2)#4–O(4)–Zn(1)	143.51(17)
O(5)–Zn(2)–O(5)#1	117.21(18)	P(1)–O(5)–Zn(2)	134.41(19)
O(5)–Zn(2)–O(1)#1	111.21(13)	P(2)–O(6)–Zn(1)	136.12(17)
O(5)#1–Zn(2)–O(1)#1	111.87(12)		

Symmetry transformations used to generate equivalent atoms: #1 $-x$, y, $-z+1/2$; #2 $-x-1/2$, $-y+5/2$, $-z$; #3 $-x-1/2$, $y-1/2$, $-z+1/2$; and #4 $-x-1/2$, $y+1/2$, $-z+1/2$.

Table 4
Atomic coordinates ($\times 10^4$) and equivalent isotropic displacement parameters (Å$^2 \times 10^3$) for **1**

	x	y	z	U (eq)
Ni(1)	5000	5924(1)	2500	12(1)
Zn(1)	2306(1)	1423(1)	1155(1)	14(1)
Zn(2)	5000	2776(1)	2500	16(1)
P(1)	4022(1)	1633(1)	379(1)	14(1)
P(2)	3070(1)	4148(1)	2387(1)	14(1)
O(1)	4045(2)	4215(3)	2323(2)	20(1)
O(2)	1140(2)	2045(4)	197(3)	28(1)
O(3)	3147(2)	1034(3)	471(3)	25(1)
O(4)	1973(2)	−230(3)	1683(2)	26(1)
O(5)	4814(2)	1748(4)	1336(2)	28(1)
O(6)	2703(2)	2701(3)	2242(2)	25(1)
C(1)	4506(3)	8792(5)	2508(4)	26(1)
C(2)	3558(5)	7493(7)	1045(4)	54(2)
C(3)	4132(7)	7085(10)	521(7)	16(2)
C(3′)	3842(9)	6469(18)	486(9)	46(4)
N(1)	4018(2)	7510(4)	2112(3)	19(1)
N(2)	4719(3)	5815(4)	994(3)	20(1)

Table 5
Atomic coordinates ($\times 10^4$) and equivalent isotropic displacement parameters (Å$^2 \times 10^3$) for **2**

	x	y	z	U (eq)
Co(1)	0	9047(1)	2500	18(1)
Zn(1)	−2696(1)	13,550(1)	1165(1)	21(1)
Zn(2)	0	12,184(1)	2500	24(1)
P(1)	−968(1)	13,323(1)	384(1)	21(1)
P(2)	−1947(1)	10,828(1)	2376(1)	21(1)
O(1)	−964(2)	10,767(2)	2329(2)	28(1)
O(2)	−3867(2)	12,978(3)	201(2)	34(1)
O(3)	−1843(2)	13,910(3)	484(2)	33(1)
O(4)	−2984(2)	15,203(2)	1709(2)	33(1)
O(5)	−181(2)	13,186(3)	1336(2)	37(1)
O(6)	−2321(2)	12,261(3)	2233(2)	33(1)
C(1)	−495(3)	6155(4)	2500(3)	33(1)
C(2)	−1334(5)	7348(6)	992(3)	76(2)
C(3)	−925(7)	7977(12)	489(6)	42(2)
C(3′)	−1209(6)	8622(8)	488(6)	26(1)
N(1)	−982(2)	7405(3)	2064(2)	26(1)
N(2)	−298(2)	9194(3)	970(2)	29(1)

approximately 2.7×8.2 Å for **1** and 2.9×8.6 Å for **2**. Furthermore, there also exist 12-MR channels along the [101], [011] and [110] directions and 8-MR channels along [011] and [110] directions. However, these channels are almost blocked by the *M*(TETA) complexes. Such multi-directional intersecting 12-MR channels are rarely observed in the inorganic–organic hybrid materials.

The TETA molecules attached to the *M* atoms locate in the channels thus reducing the free space. They interact with the inorganic framework through weak H-bonds. N(1) atom of TETA ligand forms a H-bond to bridging O(6) atom of the framework with the N(1)···O(6) distance of 3.090(5) Å for **1** and 3.088(5) Å for **2**. N(2) atom forms two weak H-bonds with O(1) and O(2), measured by using Cerius^2 software package [31]. The N(2)···O(1) and N(2)···O(2) distances are 2.978 and 3.040 Å for **1**, 2.947 and 3.015 Å for **2**, respectively.

3.3. Fluorescent spectroscopy

The photoluminescent spectra of **1**, **2** and organic amine TETA were measured at room temperature, as shown in Fig. 6. The emission spectra of **1** and **2** both exhibit one sharp peak at 423 nm and one band at 382 nm excited at 235 nm. The peaks at 423 nm of **1** and **2** are probably originated from the organic amine, as compared with the weak emission band of TETA. The similar enhanced fluorescence efficiency has been observed before [32]. The bands around 382 nm of the two compounds may be assigned to ligand-to-metal charge transfer (LMCT).

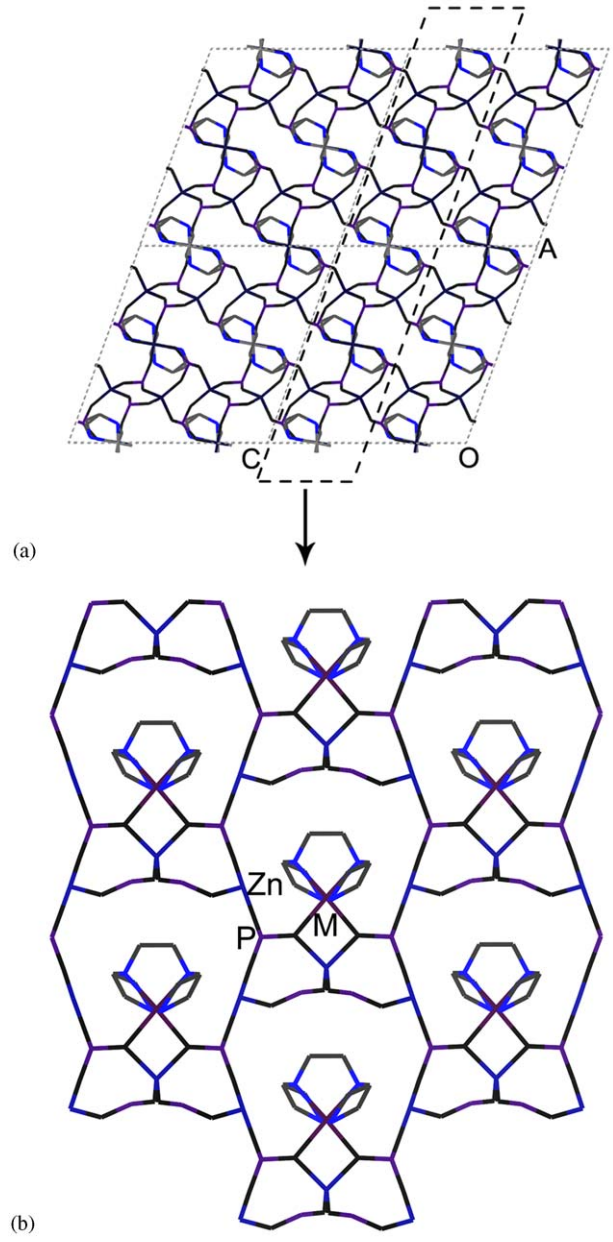

Fig. 4. (a) View of the structure of **1** and **2** along the [010] direction showing the 12-MR channels; and (b) the zinc phosphite layer of **1** and **2** with 4.12-net along the [001] direction (H atoms are omitted for clarity).

4. Conclusion

Two new inorganic–organic hybrid compounds $[Ni(C_6N_4H_{18})][Zn_3(HPO_3)_4]$ (**1**) and $[Co(C_6N_4H_{18})][Zn_3(HPO_3)_4]$ (**2**) with analogous structures have been hydrothermally synthesized. The alternating connection of ZnO_4 tetrahedra and HPO_3 pseudo-pyramids forms their 3-D open-frameworks with multi-directional intersecting 12-MR channels. The M(TETA) (M = Ni, Co) complexes locating in the channels connect with the inorganic framework through M–O–P linkages, and

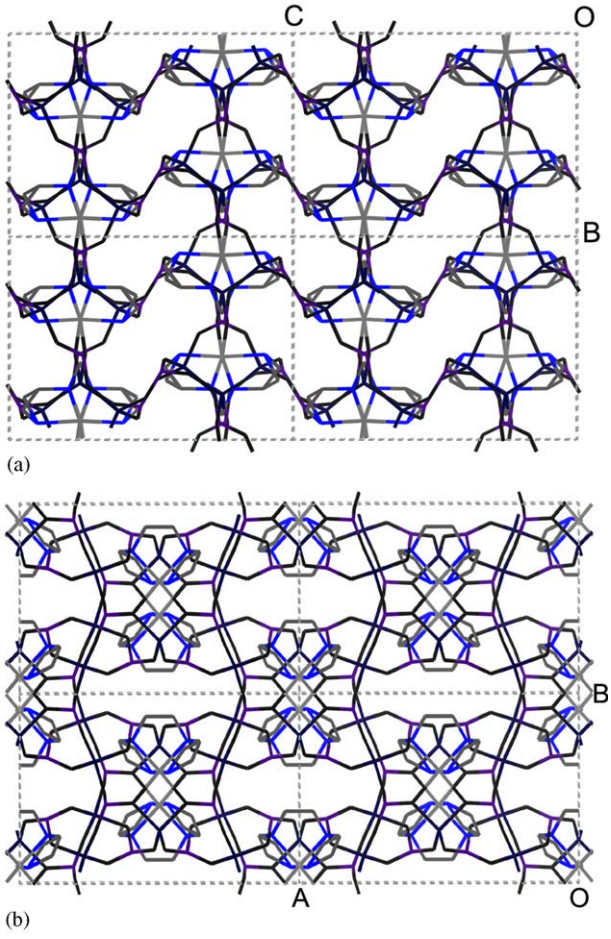

Fig. 5. View of the structure of **1** and **2** along the [100] (a) and [001] (b) directions showing the 12-MR channels (H atoms are omitted for clarity).

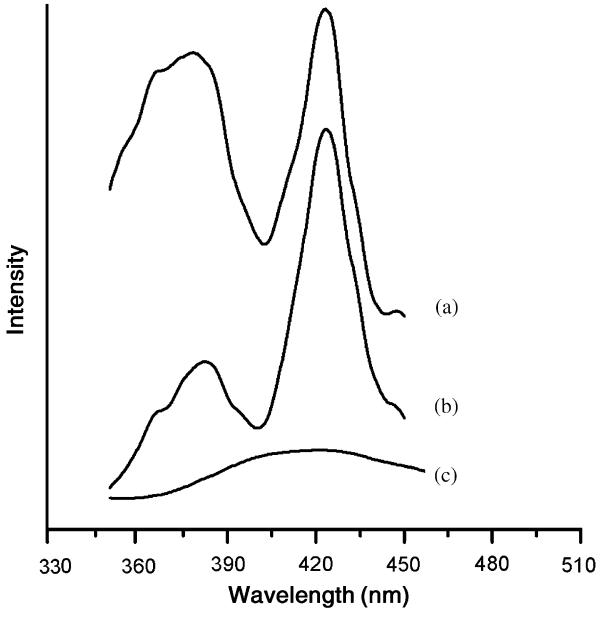

Fig. 6. The photoluminescence spectra: (a) compound **1**; (b) compound **2**; and (C) the TETA.

form weak H-bonds with inorganic framework. Fluorescent spectroscopy analysis reveals that these two zinc phosphites exhibit interesting intense photoluminescence upon photoexcitation at 235 nm.

4.1. Supporting information and structure details

Crystallographic data for the structure reported in this paper in the form of CIF file has been deposited with the Cambridge Crystallographic Data Centre as supplementary publication no.CCDC-254408 for **1** and no.CCDC-268794 for **2**. Copies of the data can be obtained free of charge on application to CCDC, 12 Union Road, Cambridge CB2 1EZ, UK (Fax: (+44)-1223-336-033; E-mail: deposit@ccdc.cam.ac.uk).

Acknowledgements

This work is supported by the National Natural Science Foundation of China and the State Basic Research Project (G20000775) of China.

References

[1] A.K. Cheetham, G. Férey, T. Loiseau, Angew. Chem. Int. Ed. 38 (1999) 3268 and references therein.
[2] C.N.R. Rao, S. Natarajan, A. Choudhury, S. Neeraj, A.A. Ayi, Acc. Chem. Res. 34 (2001) 80 and references therein.
[3] J. Yu, R. Xu, Acc. Chem. Res. 36 (2003) 481 and references therein.
[4] S.T. Wilson, B.M. Lok, C.A. Messian, T.R. Cannon, E.M. Flanigen, J. Am. Chem. Soc. 104 (1982) 1146.
[5] T.E. Gier, G.D. Stucky, Nature 349 (1991) 508.
[6] G. Yang, S.C. Sevov, J. Am. Chem. Soc. 121 (1999) 8389.
[7] J.A. Rodgers, W.T.A. Harrison, J. Mater. Chem. 10 (2000) 2853.
[8] S. Neeraj, S. Natarajan, C.N.R. Rao, Chem. Commun. (1999) 165.
[9] Y. Wang, J. Yu, M. Guo, R. Xu, Angew. Chem. Int. Ed. 42 (2003) 4089.
[10] G. Bonavia, J. Debord, R.C. Haushalter, D. Rose, J. Zubieta, Chem. Mater. 7 (1995) 1995.
[11] S. Fernandez, J.L. Pizarro, J.L. Mesa, L. Lezama, M.I. Arriortua, R. Olazcuaga, T. Rojo, Chem. Mater. 14 (2002) 2300.
[12] S. Fernandez, J.L. Mesa, J.L. Pizarro, L. Lezama, M.I. Arriortua, R. Olazcuaga, T. Rojo, Chem. Mater. 12 (2000) 2092.
[13] S. Fernandez, J.L. Mesa, J.L. Pizarro, L. Lezama, M.I. Arriortua, T. Rojo, Angew. Chem. Int. Ed. 41 (2002) 3683.
[14] W.T.A. Harrison, R.M. Yeates, M.L.F. Phillips, T.M. Nenoff, Inorg. Chem. 42 (5) (2003) 1493.
[15] W.T.A. Harrison, Int. J. Inorg. Mater. 3 (2001) 187.
[16] J. Liang, Y. Wang, J. Yu, R. Xu, Chem. Commun. (2003) 882.
[17] J.A. Rodgers, W.T.A. Harrison, Chem. Commun. (2000) 2385.
[18] W.T.A. Harrison, J. Solid State Chem. 160 (2001) 4.
[19] W.T.A. Harrison, M.L.F. Phillips, T.M. Nenoff, J. Chem. Soc., Dalton Trans. (2001) 2459.
[20] W.T.A. Harrison, M.L.F. Phillips, J. Stanchfield, T.M. Nenoff, Inorg. Chem. 40 (2001) 895.
[21] W. Fu, Z. Shi, D. Zhang, G. Li, Z. Dai, X. Chen, S. Feng, J. Solid State Chem. 174 (2003) 11.
[22] Y. Wang, J. Yu, Y. Li, Y. Du, R. Xu, L. Ye, J. Solid State Chem. 170 (2003) 303.
[23] W. Dong, G. Li, Z. Shi, W. Fu, D. Zhang, X. Chen, Z. Dai, L. Wang, S. Feng, Inorg. Chem. Commun. 6 (2003) 776.
[24] Y. Wang, J. Yu, Y. Du, Z. Shi, Y. Zou, R. Xu, J. Chem. Soc., Dalton Trans. (2002) 4060.
[25] J.M. Thomas, Y. Xu, C.R.R. Catlow, J.W. Couves, Chem. Mater. 3 (1991) 667.
[26] Z. Lin, J. Zhang, S. Zheng, G. Yang, J. Mater. Chem. 14 (2004) 1652.
[27] SMART and SAINT (software package), Siemens Analytical X-ray Instruments Inc., Madison, WI, 1996.
[28] SHELXTL, version 5.1, Siemens Industrial Automation, Inc., 1997.
[29] J. Pan, S. Zheng, G. Yang, Cryst. Growth Des. 5 (2005) 237.
[30] C.-H. Lin, S.-L. Wang, K.-H. Lii, J. Am. Chem. Soc. 123 (2001) 4649.
[31] Cerius^2, Molecular simulations/Biosym corporation, San Diego, CA, 1995.
[32] M. Fu, G. Guo, X. Liu, L. Cai, J. Huang, Inorg. Chem. Commun. 8 (2005) 18.